ARL

★ The University of Texas at Austin

TECHNICAL REPORT

Copy Number *14*

Bottom Grain Gas and Roughness Technique (BOGGART) Version 3.0: Bottom Backscatter Model User's Guide

Technical Report under Contract N00039-91-C-0082
TD No. 01A2049, Sensor and Environmental Support for MTEDS

Frank A. Boyle
Nicholas P. Chotiros

1997 0227 047

Prepared for: Naval Research Laboratory
Stennis Space Center, MS 39529-5004

Monitored by: Space and Naval Warfare Systems Command
Department of the Navy • Arlington, VA 22245-5200

DTIC QUALITY INSPECTED 3

UNCLASSIFIED

REPORT DOCUMENTATION PAGE

Form Approved
OMB No. 0704-0188

1. AGENCY USE ONLY (Leave blank)	2. REPORT DATE	3. REPORT TYPE AND DATES COVERED
	4 Jun 96	technical

4. TITLE AND SUBTITLE

Bottom Grain Gas and Roughness Technique (BOGGART) Version 3.0: Bottom Backscatter Model User's Guide, Technical Report under Contract N00039-91-C-0082, TD No. 01A2049, Sensor and Environmental Support for MTEDS

5. FUNDING NUMBERS

N00039-91-C-0082,
TD No. 01A2049

6. AUTHOR(S)

Boyle, Frank A.   Chotiros, Nicholas P.

7. PERFORMING ORGANIZATION NAMES(S) AND ADDRESS(ES)

Applied Research Laboratories
The University of Texas at Austin
P.O. Box 8029
Austin, Texas 78713-8029

8. PERFORMING ORGANIZATION REPORT NUMBER

ARL-TR-96-10

9. SPONSORING/MONITORING AGENCY NAME(S) AND ADDRESS(ES)

Naval Research Laboratory
Stennis Space Center, MS 39529-5004

Space and Naval Warfare
Systems Command
Department of the Navy
Arlington, VA 22245-5200

10. SPONSORING/MONITORING AGENCY REPORT NUMBER

11. SUPPLEMENTARY NOTES

12a. DISTRIBUTION/AVAILABILITY STATEMENT

Approved for public release; distribution is unlimited.

12b. DISTRIBUTION CODE

13. ABSTRACT (Maximum 200 words)

A user's guide has been developed for BOGGART, a model for acoustic backscatter from marine sediments, developed at Applied Research Laboratories, The University of Texas at Austin (ARL:UT), with support from the Naval Research Laboratory at Stennis Space Center (NRL/SSC). The model, named for "bottom grain gas and roughness technique," computes the total backscattering strength as an incoherent sum of contributions from three components. They are (1) scattering from sediment grains, (2) scattering from trapped gas bubbles within the sediment, and (3) scattering from interface roughness. The grain scattering is modeled semiempirically, based on the diffusion equation, in lieu of using a theoretical model which is under development. The gas bubble and roughness-scattering components are theoretical. Acoustic propagation in the sediment is modeled by way of the Biot theory for poroelastic media. This report is a user's description for BOGGART, version 3.0.

14. SUBJECT TERMS

backscatter	grains	sand
Biot theory	porous medium	seafloor
gas bubbles	roughness	sediment

15. NUMBER OF PAGES

39

16. PRICE CODE

17. SECURITY CLASSIFICATION OF REPORT	18. SECURITY CLASSIFICATION OF THIS PAGE	19. SECURITY CLASSIFICATION OF ABSTRACT	20. LIMITATION OF ABSTRACT
UNCLASSIFIED	UNCLASSIFIED	UNCLASSIFIED	SAR

NSN 7540-01-280-5500

UNCLASSIFIED

Standard Form 298 (Rev. 2-89)
Prescribed by ANSI Std. 239-18
298-102

This page intentionally left blank.

TABLE OF CONTENTS

This page intentionally left blank.

LIST OF FIGURES

This page intentionally left blank.

1. INTRODUCTION

Acoustic backscatter from the seafloor has generated considerable interest over the past several decades. The importance of seabed acoustics has recently grown because of current emphasis on mine warfare in the littoral environment. Since no general agreement currently exists on the physics of the scattering process, many models have been developed on the basis of several different hypothetical scattering mechanisms. They include models based on scattering at the sediment interface, like those of Patterson[1] and Clay and Medwin,[2] as well as the volume scattering models of Nolle,[3] Stockhausen,[4] and Ivakin and Lysanov.[5] Jackson et al.[6-8] developed a two-component model that treats interface roughness scattering and volume scattering separately. When this model is applied to several sites, it suggests that both components are important, each dominating the total backscatter prediction in three of six cases.

The Jackson et al.[6-8] model characterizes the seabed with six parameters, two of which describe the interface roughness and three of which describe acoustic propagation through the sediment, modeled as an acoustic fluid. The remaining parameter is an empirically determined quantity that specifies the level of volume scattering within the sediment. No attempt is made to specify the actual volume-scattering mechanisms involved.

In 1990, Chotiros[9] began a comprehensive compilation of all available shallow grazing angle backscatter data published in the literature. The results appear to show some statistically significant trends that suggest specific volume-scattering mechanisms that might be modeled physically. Two hypothetical scattering mechanisms, involving scattering from sediment grains and from trapped bubbles, appear to fit the general trends in the data. At present, the data set is expanding and the trends remain.

In 1992 the results of three acoustic penetration experiments at sea[10,11] and in the laboratory[12] became available. They suggest that sandy sediments might best be modeled structurally via the Biot poroelastic theory, particularly for high frequencies and shallow grazing angles.

In 1993 development of a new backscatter model[13] began that was designed to take advantage of the most recent experimental information. The resulting model is named BOGGART, an acronym for "bottom grain gas and roughness technique." BOGGART is intended for minehunting applications and is therefore optimized for shallow grazing angle, high frequency behavior. Like Jackson's model, BOGGART includes volume and interface scattering components but is different in its modeling of the sediment structure and in the modeling of scattering mechanisms.

BOGGART is unique among current scattering models in two important ways. First, the sediment is modeled structurally via the Biot theory. Second, the volume scattering is modeled physically rather than empirically. BOGGART consists of three modular components that predict partial scattering strengths that are due to sediment grains, gas bubbles, and interface roughness.

This report is intended to serve as a user's manual for BOGGART, version 3.0. Section 2 of this report is an overview of the theory. Section 3 describes BOGGART'S operation from the user's perspective.

BOGGART 3.0 differs from the previously released version 1.0 because of the following modifications: (1) A semiempirical expression for the grain-scattering component, based on the diffusion equation, replaces an earlier, purely empirical expression. The new expression is described in Section 2.2.1. (2) The input file structure has been modified to allow the user more flexibility. Originally, BOGGART required the user to specify each of the geoacoustic parameters required by the Biot model. A library of characteristic input parameters for various common sediment types was included, which the user could modify. In the current version, the user can specify a partial set of parameters, the values of which are known. BOGGART will estimate default values for the remaining parameters according to known analytical and empirical relationships.[21] This is described from a user's perspective in Section 3. (3) Numerous small changes were made in the code structure to enable compatibility with a wider set of compilers and platforms.

2. OVERVIEW OF THEORY

This section discusses the underlying concepts upon which BOGGART is built. As was stated in the introduction, BOGGART differs from other current backscatter models because it incorporates the Biot theory to describe the seabed structure and because the volume-scattering mechanisms are modeled physically rather than empirically. Section 2.1 discusses the significance of Biot theory in modeling backscatter. Section 2.2 explains BOGGART's physical scattering mechanisms. The expected ranges of validity for the input parameters are discussed in Section 2.3.

2.1 BIOT THEORY

The Biot theory differs from other sediment theories in that it treats the sediment as a two-phase medium, consisting of a solid skeletal structure of sediment grains, through which a pore fluid flows. Two compressional waves exist, one consisting of pore fluid and grains moving in phase and a second consisting of the two moving against one another out of phase. The first of these waves propagates faster and is called the Biot fast wave; the other is called the Biot slow wave. Slow waves generally attenuate rapidly in comparison with fast waves and are therefore considered negligible. In general, therefore, sediments are modeled with simpler one-phase models, such as elastic or fluid models.

Recent experiments suggest that there are important special cases in which slow waves are not negligible, making the Biot theory most applicable. In these experiments, conducted both at sea and in the laboratory, a slow acoustic wave having a sound speed near 1200 m/s was observed in sandy sediment. The wave was significant at frequencies greater than 10 kHz and grazing angles less than 20 degrees. The existence of this wave cannot be explained via fluid or elastic theories but can be modeled as a Biot slow wave with a reasonable set of input parameters.

Measurements of normal incidence reflection coefficients also suggest that sandy sediment is structured as a Biot medium. Figure 2.1 shows several such measurements, alongside theoretical values based on Biot and elastic theory. The Biot model appears to be most consistent with the measurements.
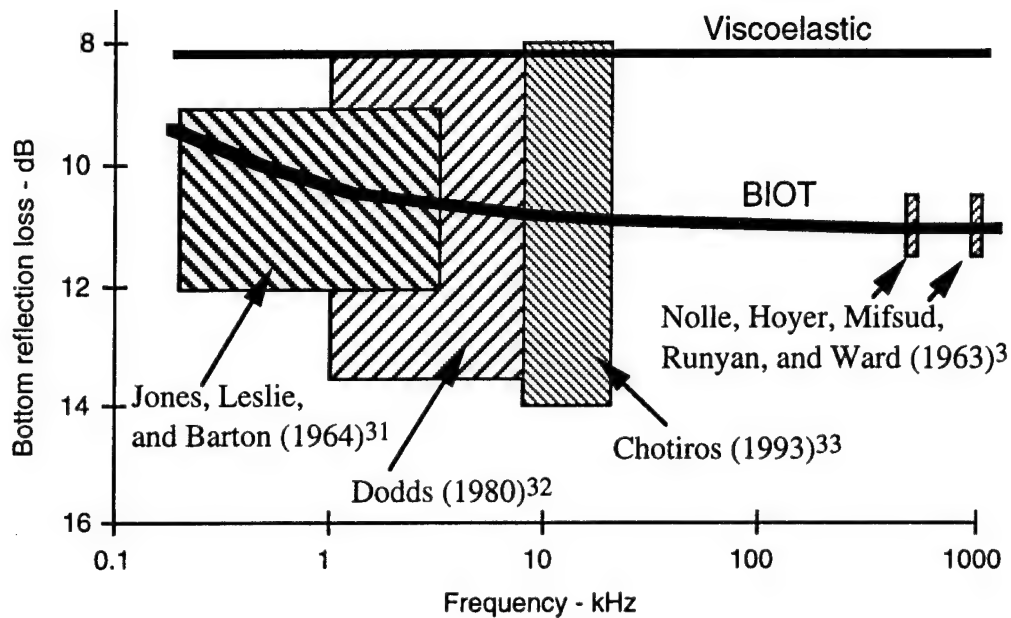
Figure 2.1
Comparison of published normal incidence refection
measurements with viscoelastic and Biot theories.

The Biot theory applied in BOGGART was originally formulated by Stern, Bedford, and Millwater.[14] Its incorporation into the model is described in Ref. 13.

2.2   SEDIMENT-SCATTERING MECHANISMS

Figure 2.2 is a plot of all shallow grazing backscatter measurements available in the literature. This collection was compiled by Chotiros[15] and includes data from the U.S.A., Canada, the U.K., and Russia, beginning with some measurements recorded by Urick in the 1950s. Each data point represents a backscattering strength measurement over sediment at a grazing angle of 10 degrees. The data spans a broad range between (1) an upper limit defined by Lambert's rule and energy conservation and (2) a lower limit defined by Nolle's experiments[16] over finely graded and degassed laboratory sands. An outstanding feature of Nolle's data is that the backscattering strength increases steadily with normalized grain size.

If the data points are grouped according to the site where they were collected, two trends appear, as shown in Fig. 2.3. In this equation, data points from a common site are connected with lines. In group 1, the backscattering strength increases with normalized grain size, just as was the case for Nolle's data[16] over degassed sands. This dependence of the scattering strength on the size of the sediment grain suggests that the grains are involved in the scattering process. In group 2, the backscattering strength appears to have a relative maximum when the grain diameter is about $10^{-2.5}$ wavelengths. This is close to the resonance diameter of gas bubbles in water, suggesting that trapped bubbles in resonance might be a dominant mechanism in the scattering process.

BOGGART's hypothesis is that the shallow grazing angle scattering data shown in Figs. 2.2 and 2.3 is dominated by two scattering mechanisms: grain scattering, which dominates the data of group 1, and bubble scattering, which dominates that of group 2. At larger grazing angles, interface roughness might become important. BOGGART models these three scattering mechanisms in separate modules, described in the following subsection.
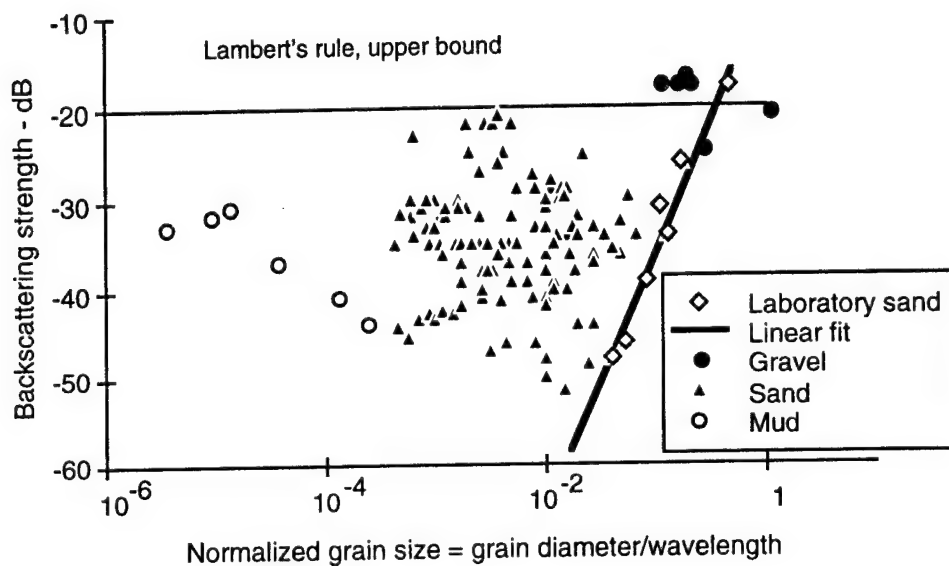
Figure 2.2
Experimental measurements of bottom backscattering
strength as a function of grain size at a grazing angle of 10°,
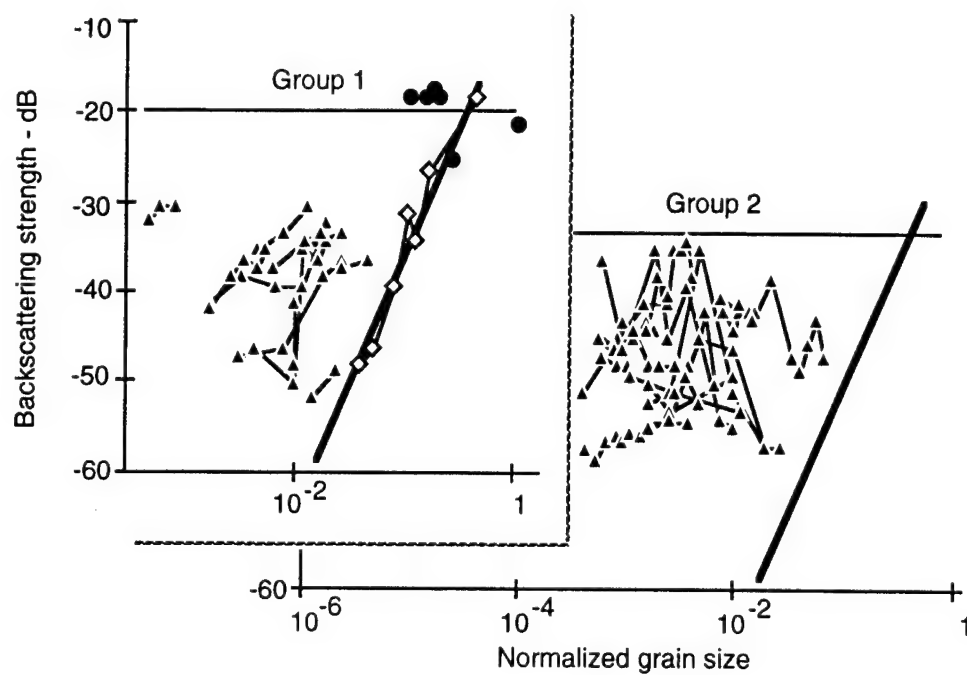**from all published sources.**

6

Figure 2.3
Experimental measurements of bottom backscattering strength as a function of grain size at a grazing angle of 10°, groups 1 and 2.

2.2.1 Sediment Grains

A theoretical model for acoustic scattering from sediment grains is currently under development.[17] This model is based on the Biot theory[18-21] for acoustic propagation through fluid-saturated porous media, with a modification that includes the effects of scattering. In lieu of a completely theoretical scattering model, a semiempirical model, based on the assumption that the scattering process falls under the multiple scattering category, was developed using the diffusion equation.[22] This model is semiempirical because experimental measurements by Nolle et al.[3] were used to compute the values of certain input parameters. The resulting expression for backscattering strength associated with direct acoustic interaction with sediment grains is given by

$$BS_g = 10 \, \mathrm{Log} \left(\frac{\alpha \, \beta \sin^2[\theta] \, \phi[\theta]}{[\gamma + \alpha \beta] \pi} \right) \tag{2.1}$$

where

θ = grazing angle;

$\phi(\theta)$ = energy transfer coefficient from water into sediment;

α = diffusivity;

β = decay coefficient of coherent acoustic energy as a function depth;

γ = absorption coefficient of diffuse acoustic energy.

2.2.2 Trapped Gas Bubbles

The trapped bubble component of the backscattering strength is based on resonance scattering from bubbles that exist in a fluid-saturated porous medium. Acoustic propagation within the medium is modeled by the Biot theory. Bubble resonance behavior inside sediment pores is modeled via a simple modification to existing theory for bubbles surrounded by unbounded fluids.[23-25] In this modification, the pore fluid is assigned an effective density that differs from its actual density and accounts for the fluid's partial confinement. The details are described in Ref. 13.

Once the bubble-scattering strength is known, an expression is developed for the backscattering strength per unit volume of sediment containing bubbles.

8

An effective sediment interface scattering strength is obtained by assuming that the backscatter is a sum of contributions from all volume elements below the interface. The resulting expression for the bubble-backscattering strength component over a unit area of sediment interface is given by

$$BS = 10 \log \left(\frac{\left(\frac{A_1}{r_{1m}^2}\right) \int_0^\infty |p_{1f} + p_{1s}|^2 \left[\frac{\sigma_{bvf}}{4\pi}\left(\frac{\rho_0 c_0}{\rho_{1f} c_{1f}}\right)|p_{1f}|^2 + \frac{\sigma_{bvs}}{4\pi}\left(\frac{\rho_0 c_0}{\rho_{1s} c_{1s}}\right)|p_{1s}|^2 \right] dz}{|p_{inc}|^4} \right) \qquad (2.2)$$

where

A_1 = unit area of sediment interface;

r_{1m} = unit radius;

σ_{bvf} = sediment volume scattering cross section - fast wave;

σ_{bvs} = sediment volume scattering cross section - slow wave;

p_{inc} = incident acoustic pressure;

p_{1f} = refracted acoustic pressure - fast wave;

p_{1s} = refracted acoustic pressure - slow wave;

ρ_0 = fluid density above sediment;

ρ_{1f} = effective pore fluid density - fast wave;

ρ_{1s} = effective pore fluid density - slow wave;

c_0 = sound speed in water column;

c_{1f} = fast wave sound speed;

c_{1s} = slow wave sound speed;

z = depth below water-sediment interface.

2.2.3 Interface Roughness

The backscatter from interface roughness is modeled by solving the Helmholz-Kirchhoff integral. In this regard, it is similar to the approach used by Jackson et al.[26] Both models make the Kirchhoff approximation, which limits the frequency range of applicability. The estimated applicable range has been estimated by Chotiros[27] for the measured roughness spectra of ocean sediments by Briggs.[28] However, the method adopted here is different from that of Jackson et al. in two important respects. (1) A numerical approach is used to compute the scattering strength as a function of grazing angle, so that the measured wavenumber spectra of roughness from real ocean sediments, expressed in the form of a structure function, may be used; whereas Jackson et al.[29] attempted to fit a linear power law to measured wavenumber spectra. As a result, their ability to model was limited because the integral would converge only within a limited range of power law slopes. (2) The Biot theory is used to determine the sediment plane wave reflection coefficient, whereas in Jackson et al. the sediment is approximated as a fluid. When compared to measured values of reflection loss from ocean sediments, the Biot theory has been shown to give more realistic results. The plane wave backscattering strength, which is a simplified version of a result developed by Chotiros for roughness scattering under more general conditions, is given by the following expression:

$$BS_r = 10 \log \left[\left| \int_{-\infty}^{\infty} \int_{-\infty}^{\infty} \left| \frac{kR}{2\pi} \sin(\theta) \right|^2 \exp\left\{ -2k^2 \left[D_z\left(\sqrt{x^2+y^2}\right) \sin^2(\theta) \right] + 2ikx\cos(\theta) \right\} dxdy \right| \right] \tag{2.3}$$

where

k = acoustic wavenumber;

θ = grazing angle;

D_z = structure function of roughness;

R = plane wave reflection coefficient, a function of the grazing angle.

2.2.4 Total Backscattering Strength

The total backscattering strength is the incoherent sum of the contributions from sediment grains, trapped bubbles, and interface roughness:

$$BS = 10 \log \left(10^{0.1\,BS_g} + 10^{0.1\,BS_b} + 10^{0.1\,BS_r}\right)$$ (2.4)

2.3 RANGE OF VALIDITY

The approximate range of validity is estimated to be as follows:

PARAMETER	RANGE
Frequency range	5 to 500 kHz
Sediment grain size	-1 to 8 ϕ
Grazing angles	2° to 87°
Water depth	> 1 m
Sediment gas concentration	< 0.0001

The underlying theory assumes a poroelastic medium having solid particles and fluid-filled pore spaces. The parameter values are known to be valid for sediments with porosities in the region of 30% to 90%, which corresponds to grain sizes from about -1 to 8 ϕ. The model is intended for high frequency sonar systems. Below about 5 kHz, interaction with sub-bottom layers will tend to dominate, and the simple, uniform half space approximation will no longer be tenable. Above about 500 kHz, depending on grain size, the underlying assumption that pore sizes are small relative to the sound wavelength, within Biot's theory, will tend to break down. Above about 100 kHz, the bubble-scattering component model will become increasingly inaccurate because non-resonance scattering is ignored. Grazing angles are limited at the low end by the lack of any provision for shadowing effects. Near normal incidence, wavefront curvature effects cannot be ignored, and the plane wave assumption becomes inappropriate.

In water depths less than 1 m, such as in a surf zone, the constant resuspension of sediment is expected to invalidate the assumption that a discrete water-sediment interface exists. There is no intrinsic upper limit on the water depth, but the default values of the bulk properties of the pore liquid are those of seawater at sea level. At depths where the water bulk properties are expected to be significantly different, the user must enter the appropriate values in the optional sediment properties file. Gas bubbles in the sediment pore water,

especially in shallow water areas, are expected to be a dominant source of backscatter. In the absence of a user-supplied gas concentration, a default value of 0.001% is used in the model. The current version is not expected to be valid for gas concentrations greater than about 0.01% because the effect of the gas bubbles on the bulk properties of the pore liquid are ignored.

3. RUNNING BOGGART

BOGGART is written in FORTRAN77. The input and output files are in ASCII format. The principle input file is "BOGGART3.inp." In addition, there must be one other file that lists the frequencies and grazing angles for which backscattering strength and forward loss computations are required. The user may provide a basic sediment description in "BOGGART3.inp," from which BOGGART will generate default values of the more detailed parameters. For the advanced user, optional input files with detailed descriptions of sediment properties, roughness, and gas profile may be used to define precisely all input parameters. BOGGART produces three output files. Input and output files are described in detail in Sections 3.1 and 3.2. An example run of BOGGART follows in Section 3.3.

3.1   INPUT

Input parameter values for BOGGART are entered via input files, which can be edited by the user using any text editor. All input files must conform to the format described in the following subsection. All units are SI metric units unless otherwise stated. The first line of each input file is a comment of up to 120 characters. The comments are carried over to an output file for user reference purposes.

3.1.1 Required Input Files

The file called "BOGGART3.inp" is the main input file that governs the program. An example is given in Fig. 3.1.

```
#Test run of BOGGART3 using default options
#Enter appropriate parameter values, or -99. for default values
'mean.grain size(phi)[N1]_____' 0.
'porosity[N1}_____' -99.
'RMS.roughness.(m)[N1]_____' 0.01
'volume.gas.fraction[N1]_____' 0.5e-5
'water.depth(m)[N1]_____' 30.
#Enter appropriate file names for input parameters and output results
'sonar.parameters.file_____' sonar.par
'site.sediment.file(optional)_____' default
'sediment.roughness.file(optional)_____' default
'sediment.gas.file(optional)_____' default
'output.file.prefix_____' test
#There will be 3 output files with the above prefix
#NNN.BSfile will contain backscattering strength vs grazing angle
#NNN.const will contain a copy of all the input parameters
#NNN.vel will contain the wave velocities in the sediment
```

Figure 3.1
Example of "BOGGART3.inp."

The file contains specific comment lines and input data lines. The comment lines are marked by "#." The user may change the first comment line. The remaining comment lines improve the readability of the file and should not be changed. Each input data line consists of a character string without comma or space characters identifying the input parameter, followed by its value. The first four data lines allow the user to specify a basic set of parameter values. The basic parameter set consists of sediment mean grain size (ϕ), porosity, RMS roughness (m), and a gas volume fraction within the pore fluid; the value of the grain size unit (ϕ) is equal to the negative $\log_2$ (grain diameter in millimeters). A value of -99 signals BOGGART to obtain the value from either an optional input file or, if no optional files are provided, to generate an appropriate default value. In this example, the mean grain size is specified as 0 ϕ. The porosity is not known. The RMS roughness is 1 cm, and the gas volume fraction is set to 0.005%.

Five more input lines allow the user to specify filenames for input and output. The first is the name of a file that provides a list of frequencies and grazing angles for computation. An example is provided in the file "sonar.par," as shown in Fig. 3.2. The first line is a comment line for the user to change. The quantity NTIMES is the number of frequencies to be selected. The frequencies will be logarithmically spaced between the minimum FS4M and the maximum FS4X, inclusive. If NTIMES equals 1, then the modeled frequency will be the

14

minimum FS4M. The quantity NTHETA is the number of grazing angles, which will be evenly spaced between the limits THETMN and THETMX. In this example, two frequencies are requested, 20 and 200 kHz. At each frequency, backscatter computations will be made at 85 evenly spaced grazing angles, between 3° and 87°. If more than two frequencies are requested, they will be logarithmically spaced.

```
#sonar parameters
'NTIMES-.NUMBER.OF.FREQUENCIES_____' 2
'FS4M-.MIN.FREQUENCY.<kHz>._____' 20.
'FS4X-.MAX.FREQUENCY.<kHz>._____' 200.
'NTHETA.-.NUMBER.OF.GRAZING.ANGLES_____' 85
'THETMN-.MIN.GRAZING.ANGLE.<DEG>._____' 3.
'THETMX-.MAX.GRAZING.ANGLE.<DEG>._____' 87.
```

Figure 3.2
Example of frequency and grazing angles file: "sonar.par."

AS-96-272

3.1.2 Optional Input Files

The next three filenames are optional. The advanced user may use these to direct BOGGART3 to files that more precisely define the sediment properties, roughness, and gas volume fraction profile. The corresponding examples are "sediment.sand," "rough.MissionBay," and "gas.layers.05," as shown in Figs. 3.3 and 3.4. In the example of Fig. 3.1, none of the optional input files are used. The last data input line allows the user to set the prefix of the output filenames. In this example, the output filenames are assigned the prefix "test."

A file containing a complete set of Biot parameters may be used to describe precisely the sediment properties. An example is shown in Fig. 3.3. The first line is a comment line for the user to change. The parameters are broken into three groups: (1) solid parameters that describe the grain material, (2) fluid parameters that describe the pore fluid, and (3) frame parameters that describe the skeletal structure of the grain matrix.

15

```
#sediment parameters: sand MGS= .62ø
Chotiros, JASA 97(1),(1995); Boyle JASA 98(1), (1995)
solid parameters
'RHOS-.SEDIMENT.GRAIN.DENSITY.<kg.m^-3>_' 2690.
'XKR-..SEDIMENT.GRAIN.BULK.MOD.<Pa>____' 7.e9
'MEAN.GRAIN.PHI<MPHIs>_____' 0.62
'STAND.DEV.PHI<SIGPHIs>_____' 0.95
#
#fluid parameters
'cpf-SPEC.HEAT.OF.FLUID.CONST.PRESSURE__' 3.89e3
'ckf-HEAT.CONDUCTIVITY.FLUID_____' 0.629
'RHOF-.UPPER.FLUID.DENSITY.<kg.m^-3>____' 1023
'XKF0-.UPPER.FLUID.BULK.MOD.<Pa>_____' 2.25e9
'RHOFBLO-.PORE.LIQUID.DENSITY.<kg.m^-3>_' 1023
'XKF0BLO-.PORE.LIQUID.BULK.MODULUS.<Pa>_' 2.25e9
'ETA-..PORE.LIQUID.VISCOSITY.<kg.m^-1.s>' 1.00e-3
'WATER.DEPTH<M>_____' 60.
#
#frame parameters
'rkoz-...KOZENY.PARAMETER..(-)_____' 5.0
'rvm-...VIRTUAL.MASS.RATIO.(-)_____' 0.5
'B-....SEDIMENT.POROSITY.<->_____' .401
'XMU0-.SEDIMENT.FRAME.SHEAR.MOD..<Pa>___' .261e+8
'DMU0-.SEDIMENT.FRAME.SHEAR.LOG.DECR.<->' .15
'XKB0-.SEDIMENT.FRAME.BULK.MOD.<Pa>_____' 5.3e9
'DKB0-.SEDIMENT.FRAME.BULK.LOG.DECR..<->' .15
```

Figure 3.3
Example of sediment properties file: "sediment.sand."

The roughness of the sediment surface may be more precisely described by means of a structure function. Only an isotropic structure function is allowed at present. An example is shown in Fig. 3.4. The first line is a comment line for the user to change. The second line gives the number of structure function samples. Each sample consists of a pair of numbers: the separation (m) and the corresponding structure function value (m^2).

```
#Sand:Briggs OCEAN ENG 1989 14(4),Mission Bay II (isotropic)
26          ! number of structure function samples in look up table
0   0
0.00032922        2.5365E-09
0.00049383        5.6758E-09
0.00074074        1.2616E-08
0.00111111        2.7638E-08
0.00166667        5.88E-08
0.0025            1.1877E-07
0.00375           2.2481E-07
0.005625          4.1234E-07
0.0084375         7.5914E-07
0.01265625        1.3663E-06
0.01898438        2.3644E-06
0.02847656        3.8765E-06
0.04271484        5.897E-06
0.06407227        8.2724E-06
0.0961084         1.1138E-05
0.1441626         1.5345E-05
0.2162439         2.1896E-05
0.32436584        3.1934E-05
0.48654877        4.6889E-05
0.72982315        6.8196E-05
1.09473473        9.6382E-05
1.64210209        0.00012911
2.46315313        0.00015898
3.6947297         0.000176
5.54209455        0.00017976
```

Figure 3.4
Example of sediment roughness file: "rough.MissionBay."

AS-96-274

The sediment gas profile may be described in detail in a separate file, as shown in the example in Fig. 3.5. The first line is a comment line for the user to change. The parameters include specific heat at constant pressure, heat conductivity, density, and bulk modulus. The last line is equal to atmospheric pressure at sea level multiplied by the ratio of specific heats. These constants are followed by the gas volume fraction profile. The gas profile is modeled as a series of consecutive constant volume fraction layers. Each entry contains the depth below the sediment surface (m) of the top of a layer and its gas volume fraction. As many as 20 entries may be used.

```
#gas parameters at sea level(SI units) : air
'cpg-SPEC.HEAT.OF.GAS..CONST.PRESSURE__' 1.00e3
'ckg-HEAT.CONDUCTIVITY.GAS_____' 0.023
'rhog-GAS.DENSITY.<kg.m^-3>_____' 1.22
'XKG-..GAS.BULK.MOD..<Pa>_____' 1.34e5
'DEPTH.OF.TOP.OF.LAYER.(M),GAS.FRACTION:'
0.,1E-15
0.055,1E-5
0.8,1E-15
```

Figure 3.5
Example of sediment gas profile file: "gas.layers.05."

3.2   OUTPUT FILES

BOGGART produces three output files. The filenames consist of a prefix, specified by the user in the BOGGART3.inp file, and the suffix ".const," ".BS," or ".vel."

The "nnn.const" file is a read-back of BOGGART's input parameters. An example is given in Fig. 3.6. The purpose of this file is to provide a complete record of the input parameter values. In this example, BOGGART3 has given the sediment a porosity of 35%, using an empirical relationship from Hamilton.[30] All the other sediment parameters are computed using default relationships. A default roughness structure function and a default gas concentration profile is built in on the basis of experimental data. If the user specifies only an RMS roughness, the default structure function is scaled to comply. If the user specifies only a gas concentration, the default gas profile is scaled to comply, so that the maximum gas concentration is equal to the specified value. Gas properties, such as density and bulk modulus, are specified at sea level, and BOGGART scales them to the specified depth.

```
Program BOGGART3
#Test run of BOGGART3 using default options
sonar parameter input file_____ sonar.par
sediment property file_____ default
sediment roughness file_____ default
sediment gas file_____ default
output file _____ test

No sediment file: use built-in default parameters
No roughness file: use built-in default structure
No gas file: use built-in default gas profile
sediment parameters:
Default sediment parameters for generic sediment
solid parameters
RHOS-.SEDIMENT.GRAIN.DENSITY.(kg.m^-3)_  2650.00
XKR-..SEDIMENT.GRAIN.BULK.MOD.(Pa)_____  9.250000E+09
MEAN.GRAIN.PHI(rphis)_____  .000000
STAND.DEV.PHI(dphis)_____  1.09524

fluid parameters
jhcpf-SPEC.HEAT.OF.FLUID.CONST.PRESSURE  3890.00
jhckf-HEAT.CONDUCTIVITY.FLUID_____  .629000
RHOF-.UPPER.FLUID.DENSITY.(kg.m^-3)____  1023.00
XKF0-.UPPER.FLUID.BULK.MOD.(Pa)_____  2.250000E+09
RHOFBLO-.PORE.LIQUID.DENSITY.(kg.m^-3)_  1023.00
XKF0BLO-.PORE.LIQUID.BULK.MODULUS.(Pa)_  2.250000E+09
ETA-..PORE.LIQUID.VISCOSITY.(kg.m^-1.s)  1.000000E-03
WATER.DEPTH_____  30.0000

frame parameters
rkoz-...KOZENY.PARAMETER..(-)_____  5.00000
rvm-...VIRTUAL.MASS.RATIO.(-)_____  .500000
B-....SEDIMENT.POROSITY.(-)_____  .350000
XMU0-.SEDIMENT.FRAME.SHEAR.MOD..(Pa)__  7.250481E+07
DMU0-.SEDIMENT.FRAME.SHEAR.LOG.DECR.(-)  .150000
XKB0-.SEDIMENT.FRAME.BULK.MOD.(Pa)_____  7.250481E+09
DKB0-.SEDIMENT.FRAME.BULK.LOG.DECR..(-)  .150000

dependent constants
Vbp_____  1.03562
VMASS-..VIRTUAL.MASS.CONSTANT.(-)_____  1.92857
PERM-...PERMEABILITY(m^2)_____  1.784534E-09
aa-....PORE.SIZE.PARAMETER.(m)_____  3.193327E-04
CC-....CONSTITUTIVE.PARAMETER.C____  (1.538478E+09,2.211457E+08)
CH-....CONSTITUTIVE.PARAMETER.H____  (7.671441E+09,-2.454189E+08)
CM-....CONSTITUTIVE.PARAMETER.M____  (7.082009E+09,-2.030929E+08)

Sonar parameters
#sonar parameters
NTIMES-NUMBER.OF.FREQUENCIES_____  2
FS4M-MINIMUM.FREQUENCY(kHz)_____  20.0000
FS4X-MAXIMUM.FREQUENCY(kHz)_____  200.000
NTHETA.-NUMBER.OF.GRAZING.ANGLES_____  85
THETMN.-MINIMUM.GRAZING.ANGLE.DEG_____  3.00000
THETMX.-MAXIMUM.GRAZING.ANGLE.DEG_____  87.0000
```

Figure 3.6
Example of a "nnn.const" file: "test.const."

```
Gas parameters
Default gas profile: air bubbles between 5 and 80 cm
scaled to user specified gas fraction
cpg-SPEC.HEAT.OF.GAS..CONST.PRESSURE___     1000.00
ckg-HEAT.CONDUCTIVITY.GAS_____     2.30000E-02
rhog-GAS.DENSITY.(kg.m^-3).SEA.LEVEL___     1.22000
XKG-..GAS.BULK.MOD..(Pa)..SEA.LEVEL____     134000.
number of gas profile layers___   3
     .000000   5.000000E-16
    5.000000E-02   5.000000E-06
     .800000   5.000000E-16


Roughness parameters
Default roughness: Briggs OCEAN ENG 1989 14(4) arafura sea (mud)
scaled to user specified RMS roughness
RMS.roughness(m)_____   1.000000E-02
Structure function (m,m^2)
number of structure function samples___   25
     .000000    .000000
    2.603100E-04   1.961515E-08
    3.644300E-04   3.755575E-08
    5.102000E-04   7.039345E-08
    7.142900E-04   1.270082E-07
    1.000000E-03   2.153250E-07
    1.400000E-03   3.363926E-07
    1.960000E-03   4.941197E-07
    2.744000E-03   7.278433E-07
    3.841600E-03   1.098838E-06
    5.378240E-03   1.664658E-06
    7.529540E-03   2.519501E-06
    1.054135E-02   3.817563E-06
    1.475789E-02   5.779251E-06
    2.066105E-02   8.729229E-06
    2.892547E-02   1.313302E-05
    4.049565E-02   1.963754E-05
    5.669391E-02   2.910633E-05
    7.937148E-02   4.260353E-05
     .111120   6.126560E-05
     .155568   8.591820E-05
     .217795   1.162721E-04
     .304913   1.496341E-04
     .426879   1.800086E-04
     .597630   2.000000E-04
```

Figure 3.6
Example of a "nnn.const" file: "test.const."
(cont'd)

The "nnn.BS" file is a table of computed forward loss and backscattering strengths as a function of grazing angle and frequency (Fig. 3.7). The first four lines are a list of the input files. The next two are a header, followed by the data, which are arranged in columns. The first column is the acoustic frequency in kilohertz. The second is the grazing angle in degrees. The third and fourth columns are the forward loss and phase shift. The next four columns are backscattering strengths in decibels; the fifth column is the total predicted backscattering strength, followed by the individual backscattering strength components for trapped gas bubbles, sediment grain, and interface roughness scattering. In the ninth column, the dominant scattering mechanism is identified as "gas," grains," or "roughness."

The "nnn.vel" file, shown in Fig. 3.8, is a list of computed sound speeds and attenuations within the sediment. They are based on the Biot theory and therefore include values for fast, slow, and shear waves. The purpose of this file is to provide acoustic wave speeds and attenuations within the sediment that may be useful in understanding the paths by which the sound energy engages the scattering mechanisms.

3.3   EXAMPLE RESULTS

The forward loss predictions in file "test.BS" are plotted in Fig. 3.9. The values for 20 and 200 kHz are almost identical. Both curves have a plateau in the region between 10° and 40° at a value of about -6 dB. This result is peculiar to Biot's theory; the loss in this region is mainly caused by the slow wave.

The backscattering strength plots for 20 and 200 kHz are shown in Figs. 3.10 and 3.11, respectively. In both plots, the total backscattering strength and the contributions from the three scattering mechanisms are shown. In the 20-kHz case, from 0° to 14° and again from 57° to 67°, the multiple scattering from the sediments grains is the dominant mechanism; from 14° to 56° the scattering from the sediment gas bubbles is dominant. Above 67°, scattering from the sediment roughness is dominant. Notice that the model for roughness scattering tends to be rather erratic at low grazing angles, in this case, below 40°. This is a weakness in the model, but it is not considered to be a significant

```
Program BOGGART3
    #Test run of BOGGART3 using default options
    sonar parameter input file_____ sonar.par
    sediment property file_____ default
    sediment roughness file_____ default
    sediment gas file_____ default
    output file _____ test
    FREQ   |G ANGL|FORWARD    |  BACKSCATTERING STRENGTH(dB)
    kHz   | deg  LOSS dB   deg.   TOTAL    GAS   GRAINS   ROUGH MAX
      20.000  3.0   -1.46   17.82  -47.06  -51.17  -49.19 -100.00 GRAINS
      20.000  4.0   -1.93   23.75  -43.19  -46.73  -45.72 -100.00 GRAINS
      20.000  5.0   -2.37   29.67  -40.25  -43.41  -43.11 -100.00 GRAINS
      20.000  6.0   -2.79   35.57  -37.84  -40.68  -41.03 -100.00 GAS
      20.000  7.0   -3.19   41.43  -35.92  -38.57  -39.31 -100.00 GAS
        etc...
      20.000 85.0   -9.61     .01   -6.40  -23.96  -25.10    -6.54 ROUGHNESS
      20.000 86.0   -9.61     .01   -4.55  -23.96  -25.10    -4.64 ROUGHNESS
      20.000 87.0   -9.61     .01   -2.64  -23.95  -25.09    -2.70 ROUGHNESS
    FREQ   |G ANGL|FORWARD|  BACKSCATTERING STRENGTH(dB)
    kHz   | deg  LOSS dB   deg.   TOTAL    GAS   GRAINS   ROUGH X
     200.000  3.0   -1.48   17.78  -37.01  -81.23  -37.01 -100.00 GRAINS
     200.000  4.0   -1.95   23.70  -33.54  -76.81  -33.54 -100.00 GRAINS
     200.000 80.0   -9.60    -.09   -6.80  -45.66   -7.79  -13.69 GRAINS
     200.000 81.0   -9.61    -.09   -6.72  -45.67   -7.77  -13.43 GRAINS
        etc....
     200.000 81.0   -9.61    -.09   -6.72  -45.67   -7.77  -13.43 GRAINS
     200.000 82.0   -9.61    -.08   -6.66  -45.67   -7.75  -13.20 GRAINS
     200.000 83.0   -9.62    -.08   -6.60  -45.67   -7.73  -12.99 GRAINS
     200.000 84.0   -9.62    -.08   -6.54  -45.67   -7.71  -12.82 GRAINS
     200.000 85.0   -9.62    -.08   -6.49  -45.67   -7.70  -12.66 GRAINS
     200.000 86.0   -9.63    -.08   -6.46  -45.67   -7.68  -12.54 GRAINS
     200.000 87.0   -9.63    -.08   -6.42  -45.67   -7.67  -12.44 GRAINS
```

Figure 3.7
An example of the "nnn.BS" file: "test.BS."

22

```
Program BOGGART3
#Test run of BOGGART3 using default options
Biot waves: speeds and attenuations


at FREQUENCY =   20.0000kHz:

upper.liquid.wavespeed(V)_____    1483.04 m/s(atten=0)
fast.wavespeed(VEL1o)_____     1968.81 m/s
slow.wavespeed(VEL2o)_____     1112.70 m/s
shear.wavespeed(VELso)_____     195.627 m/s
fast.absorption(ABSRP1o)_____     12.4690 dB/m
slow.absorption(ABSRP2o)_____     24.0392 dB/m
shear.absorption(ABSRPSo)_____     137.438 dB/m


at FREQUENCY =   200.000kHz:

upper.liquid.wavespeed(V)_____    1483.04 m/s(atten=0)
fast.wavespeed(VEL1o)_____     1969.85 m/s
slow.wavespeed(VEL2o)_____     1118.68 m/s
shear.wavespeed(VELso)_____     195.730 m/s
fast.absorption(ABSRP1o)_____     122.831 dB/m
slow.absorption(ABSRP2o)_____     183.361 dB/m
shear.absorption(ABSRPSo)_____     1344.25 dB/m
```

Figure 3.8
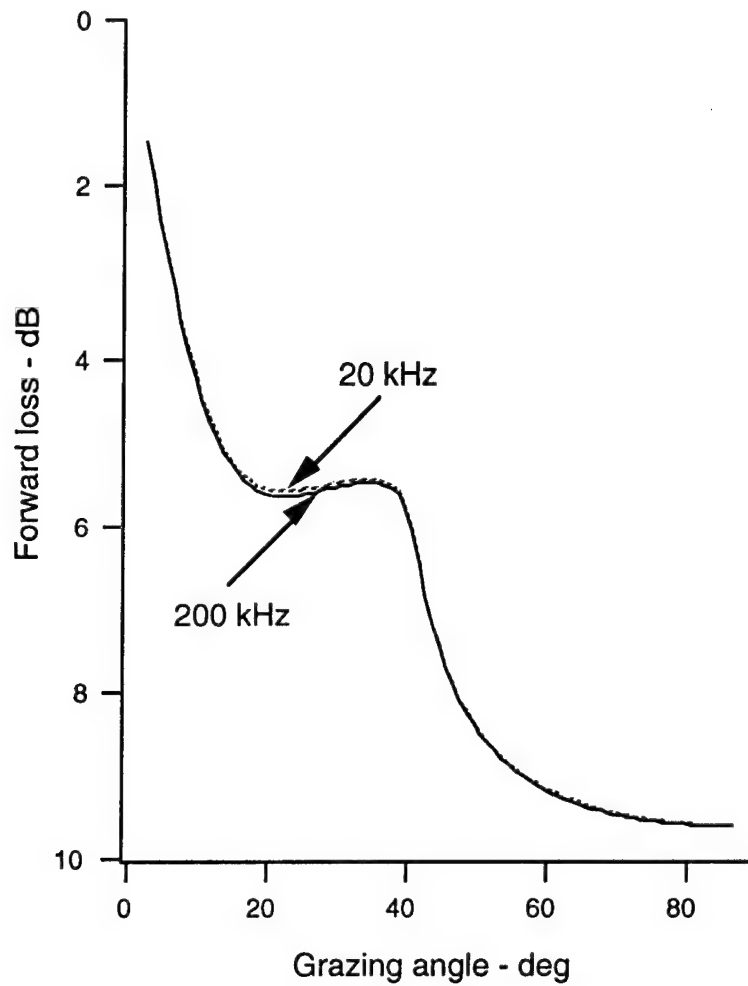**Example of "nnn.vel" file: "test.vel."**

AS-96-278

23

Figure 3.9
Forward loss values as a function of
grazing angle at 20 and 200 kHz.
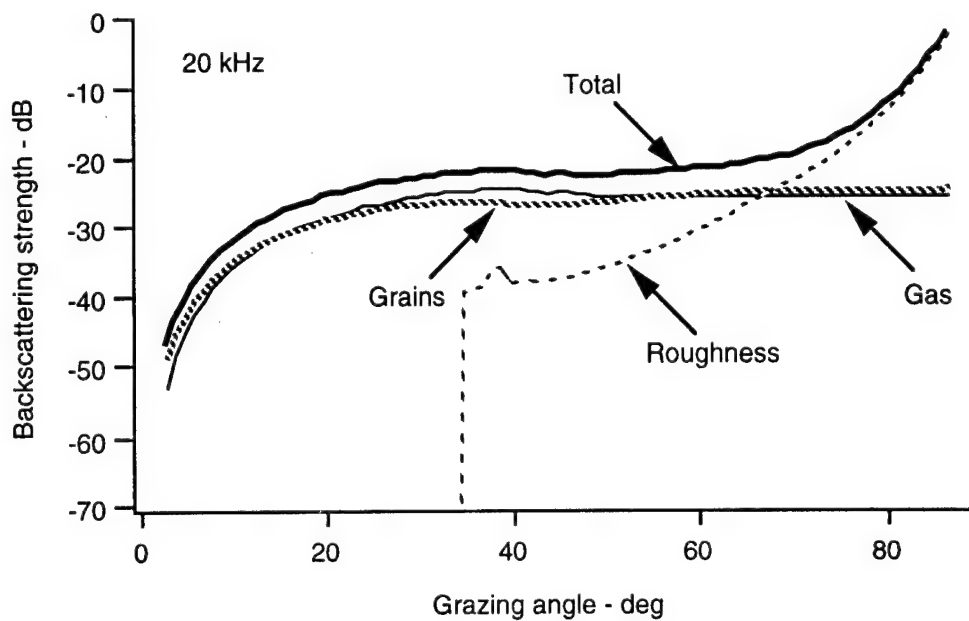
**Figure 3.10
Bottom backscattering strength plotted from
the results in "test.BS" at 20 kHz.**
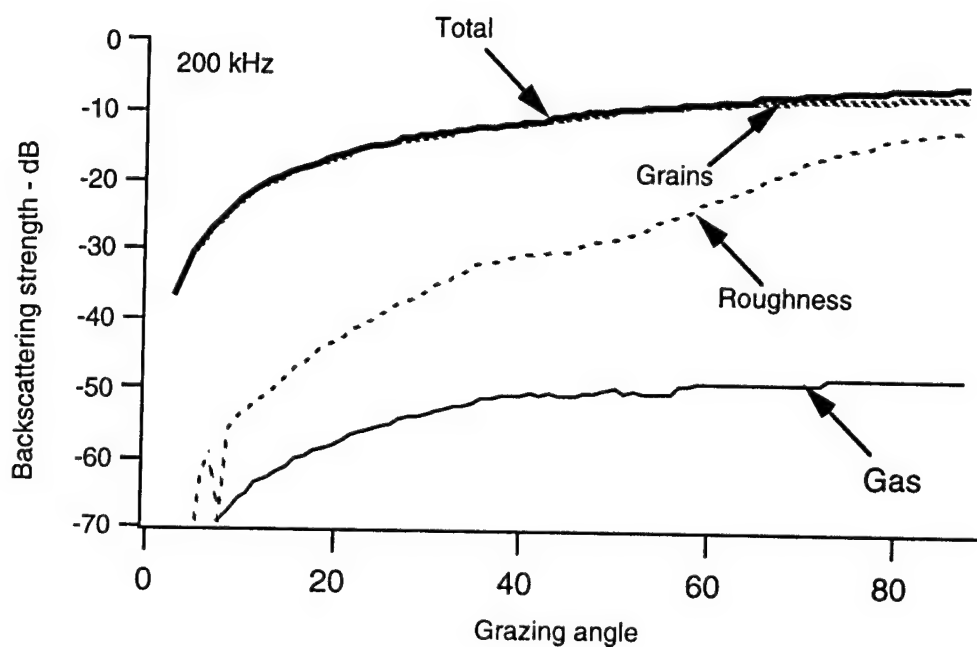
Figure 3.11
Bottom backscattering strength plotted from
the results in "test.BS" at 200 kHz.

26

problem because roughness is not the dominant scattering mechanism at shallow grazing angles. In the case of the 200-kHz signal, as shown in Fig. 3.11, the scattering by the sediment grains is predicted to be dominant at all angles computed, i.e., from 3° to 87°.

This page intentionally left blank.

ACKNOWLEDGMENTS

This page intentionally left blank.

REFERENCES

1. R. E. Patterson, "Backscatter of Sound from a Rough Boundary," J. Acoust. Soc. Am. **35,** 2010-2013 (1963).

2. C. S. Clay and H. Medwin, *Acoustical Oceanography: Principles and Applications* (Wiley-Interscience, New York, 1977).

3. A. W. Nolle, W. A. Hoyer, J. F. Mifsud, W. R. Runyan, and M. B. Ward, "Acoustic Properties of Water-Filled Sands," J. Acoust. Soc. Am. **35,** 1394 (1963).

4. J. H. Stockhausen, "Scattering from the Volume of an Inhomogeneous Half-Space," Naval Research Establishment (Canada) Report No. 63/9 (1963).

5. A. N. Ivakin and Yu. P. Lysanov, "Underwater Sound Scattering by Volume Inhomogeneities of a Bottom Medium Bounded by a Rough Surface," Sov. Phys. Acoust. **27,** 212-215 (1981).

6. D. R. Jackson, D. P. Winebrenner, and A. Ishimaru, "Application of the Composite Roughness Model to High-Frequency Bottom Backscattering," J. Acoust. Soc. Am. **79,** 1410-1422 (1986).

7. P. D. Mourad and D. R. Jackson, "High-Frequency Sonar Equation Models for Bottom Backscatter and Forward Loss," in *Proceedings of Oceans '89* (Marine Technology Society and IEEE, 1989), pp. 1168-1175.

8. D. R. Jackson and K. B. Briggs, "High-Frequency Bottom Backscattering: Roughness versus Interface Scattering," J. Acoust. Soc. Am. **92,** 962-977 (1992).

9. N. P. Chotiros and F. A. Boyle, "Gas Bubbles in Ocean Sediments and High-Frequency Acoustic Backscattering Strength," presented at 121st Meeting of the Acoustical Society of America: J. Acoust. Soc. Am. **89**(4), Pt. 2, 1852 (1991).

10. N. P. Chotiros and H. Boehme, "Analysis of Bottom Backscatter Data from the Kings Bay Experiment," Applied Research Laboratories Technical Report No. 88-6 (ARL-TR-88-6), Applied Research Laboratories, The University of Texas at Austin (1988).

11. N. P. Chotiros, "High Frequency Bottom Backscattering: Panama City Experiment," Applied Research Laboratories Technical Report No. 90-22 (ARL-TR-90-22), Applied Research Laboratories, The University of Texas at Austin (1990).

12. F. A. Boyle and N. P. Chotiros, "Experimental Detection of a Slow Acoustic Wave in Sediment at Shallow Grazing Angles," J. Acoust. Soc. Am. **91**, 2615-2619 (1992).

13. F. A. Boyle and N. P. Chotiros, "A Model for High-Frequency Acoustic Backscatter from Gas Bubbles in Sandy Sediments at Shallow Grazing Angles," J. Acoust. Soc. Am. **98**(1), 531-541 (1995).

14. M. Stern, A. Bedford, and H. R. Millwater, "Wave Reflection from a Sediment Layer with Depth-Dependent Properties," J. Acoust. Soc. Am. **77**, 1781-1788 (1985).

15. See Ref. 9.

16. See Ref. 3.

17. D. J. Yelton and N. P. Chotiros, "New Multiple Scatter Model of the Ocean Sediment," presented at 129th Meeting of the Acoustical Society of America: J. Acoust. Soc. Am. **97**(5), Pt. 2, 3387 (1995).

18. M. A. Biot, "Theory of Propagation of Elastic Waves in a Fluid Saturated Porous Solid. I. Low Frequency Range," J. Acoust. Soc. Am. **28**, 168-178 (1956).

19. M. A. Biot, "Theory of Propagation of Elastic Waves in a Fluid Saturated Porous Solid. II. Higher Frequency Range," J. Acoust. Soc. Am **28**, 179-191 (1956).

20. See Ref. 14.

21. N. P. Chotiros, "Biot Model of Sound Propagation in Water-Saturated Sand," J. Acoust. Soc. Am. **97**(1), 199-214 (1994).

22. N. P. Chotiros, A. M. Mautner, and J. Laughlin, "Backscatter Analysis from a Smooth Sand Surface: Diffusion Approximation," Applied Research Laboratories Technical Report No. 95-30 (ARL-TR-95-30), Applied Research Laboratories, The University of Texas at Austin (1995).

23. M. Minnaert, "On Musical Air Bubbles and the Sounds of Running Water," Phil. Mag. **26**, 235 (1933).

24. C. Devin, "Survey of Thermal, Radiation, and Viscous Damping of Pulsating Air Bubbles in Water," J. Acoust. Soc. Am. **31**, 1654-1667 (1959).

25. See Ref. 2.

26. See Ref. 6.

27. N. P. Chotiros, "Reflection and Reverberaton in Normal Incidence Echo-Sounding," J. Acoust. Soc. Am. **96**(5), 2921-2929 (1994).

28. K. B. Briggs, "Microtopographical Roughness of Shallow-Water Continental Shelves," IEEE J. Oceanic Eng., **14**(4), 360-367 (1989).

29. See Ref. 6.

30. E. L. Hamilton, "Geoacoustic Modeling of the Sea Floor," J. Acoust. Soc. Am. **68**, 1313-1340 (1980).

Note: The following references appear only in Fig. 21:

31.   J. L. Jones, C. B. Leslie, and L. E. Barton, "Acoustic Characteristics of Underwater Bottoms," J. Acoust. Soc. Am. **36**(1) 154-157 (1964).

32.   D. J. Dodds, "Attenuation Estimates from High Resolution Subbottom Profiler Echoes," in *Bottom-Interacting Ocean Acoustics*, W. A. Kuperman, and F. B. Jensen (eds.), NATO Conference Series IV (Marine Sciences, Plenum Press, New York, 1980), pp. 525-540.

33.   N. P. Chotiros, "Inversion and Sandy Ocean Sediments," in *Full Field Inversion Methods in Ocean and Seismo-Acoustics*, O. Diachok, A. Caiti, P. Gerstoft, and H. Schmidt (eds.), pp. 353-357, *Modern Approaches in Geophysics*, Vol. XII (Kluwer Academic Publishers, Dordrecht, 1995), pp. 353-357.

DISTRIBUTION LIST
ARL-TR-96-10
**Technical Report under Contract N00039-91-C-0082,
TD No. 01A2049, Sensor and Environmental Support for MTEDS**

<u>Copy No.</u>

	Commanding Officer
	Naval Research Laboratory
	Stennis Space Center, MS 39529-5004
1 - 3	Attn: S. Tooma (Code 7430)
4	D. Lott (Code 7431)
5	E. Franchi (Code 7100)
6	S. Stanic (Code 7174)
7	D. Ramsdale (Code 7170)
8	M. Richardson (Code 7431)
9	R. Meredith (Code 7174)
10	Library (Code 7032.2)

	Office of Naval Research
	San Diego Regional Office
	4520 Executive Drive, Suite 300
	San Diego, CA 92121-3019
11	Attn: J. Starcher, ACO

	Director
	Naval Research Laboratory
	Washington, DC 20375
12	Attn: Code 2627
13	B. Houston (Code 5136)

	DTIC-OCC
	Defense Technical Information Center
	8725 John J. Kingman Road, Suite 0944
	Fort Belvoir, VA 22060-6218
14 - 25	Attn: Library

Distribution List for ARL-TR-96-10 under Contract N00039-91-C-0082, TD No. 01A2049 (cont'd)

<u>Copy No.</u>

Director
Research Program Department
Office of Naval Research
Ballston Tower One
800 North Quincy Street
Arlington, VA 22217-5660

26	Attn: J. Simmen (Code 321)
27	E. Chaika (Code 322)
28	R. Jacobson (Code 321)
29	T. Goldsberry (Code 32)
30	D. Houser (Code 333)
31	D. Todoroff (Code 322)

Commander
Naval Meteorology and Oceanography Command
1020 Balch Boulevard
Stennis Space Center, MS 39529

32	Attn: D. Durham (Code N5A)
33	R. Martin (Code N5C)

Commander
Program Executive Office - Mine Warfare
Crystal Plaza Bldg 6
2531 Jefferson Davis Highway
Arlington, VA 22242-5167

34	Attn: J. Grembi (MIW-ID)
35	D. Gaarde (PMO407B)

G & C Systems Manager
MK48/ADCAP Program Office
National Center 2
2521 Jefferson Davis Highway, 12W32
Arlington, VA 22202

36	Attn: H. Grunin (PMO402E1)

Program Manager
MK50 Torpedo Program Office
Crystal Park 1
2011 Crystal Drive, Suite 1102
Arlington, VA 22202

37	Attn: PMO406B

Distribution List for ARL-TR-96-10 under Contract N00039-91-C-0082, TD No. 01A2049 (cont'd)

<u>Copy No.</u>

Commander
Dahlgren Division
Naval Surface Warfare Center
Dahlgren, VA 22448-5000
38   Attn: Library

Director
Applied Physics Laboratory
The University of Washington
1013 NE 40th Street
Seattle, WA 98105
39   Attn: R. Spindel
40   D. Jackson
41   K. Williams
42   S. Kargl

Director
Life Sciences Directorate
Office of Naval Research
Arlington, VA 22217-5660
43   Attn: S. Zornetzer (Code 114)

Director
Marine Physical Laboratory
The University of California, San Diego
San Diego, CA 92152
44   Attn: K. Watson
45   C. De Moustier

Commander
Mine Warfare Command
325 Fifth Street SE
Corpus Christi, TX 78419-5032
46   Attn: G. Pollitt (Code N02R)

Distribution List for ARL-TR-96-10 under Contract N00039-91-C-0082, TD No. 01A2049 (cont'd)

<u>Copy No.</u>

	Applied Research Laboratory
	The Pennsylvania State University
	P.O. Box 30
	State College, PA 16804-0030
47	Attn: R. Hettche
48	R. Goodman
49	E. Liszka
50	Library
51	D. McCammon
52	F. Symons

Commanding Officer
Coastal Systems Station, Dahlgren Division
Naval Surface Warfare Center
Panama City, FL 32407-5000
53   Attn: M. Hauser (Code 10CD)
54   R. Lim (Code 130B)
55   E. Linsenmeyer (Code 10P)

Commander
Naval Undersea Warfare Center Division
New London, CT 06320-5594
56   Attn: J. Chester (Code 3112)
57   P. Koenig (Code 33A)

Commander
Naval Undersea Warfare Center Division
Newport, RI 02841-5047
58   Attn: J. Kelly (Code 821)
59   F. Aidala (Code 842)
60   W. Gozdz (Code 843)

National Center for Physical Acoustics
University of Mississippi
Coliseum Drive
University, MS 38677
61   Attn: J. Sabatier

Physics Department
The University of Texas at Austin
Austin, TX 78712
62   Attn: T. Griffy

Distribution List for ARL-TR-96-10 under Contract N00039-91-C-0082, TD No. 01A2049 (cont'd)

<u>Copy No.</u>

	Aerospace Engineering Department The University of Texas at Austin Austin, TX 78712
63	Attn: M. Bedford
64	M. Stern
65	Robert A. Altenburg, ARL:UT
66	Frank A. Boyle, ARL:UT
67	Nicholas P. Chotiros, ARL:UT
68	John M. Huckabay, ARL:UT
69	Thomas G. Muir, ARL:UT
70	Library, ARL:UT
71 - 75	Reserve, Advanced Sonar Group, ARL:UT